AGU PUBLICATIONS

Geophysical Research Letters

RESEARCH LETTER

10.1002/2017GL075720

Key Points:

- Pyrite-structured FeO_2Hx is stable in the Fe-H_2O system at >78 GPa, ~2,000 K
- Large amount of water might have been introduced into depths during the accretion and separation of the metallic core
- Extensive reaction between water and iron might occur at the core-mantle boundary

Supporting Information:

- Supporting Information S1

Correspondence to:

L. Yuan,
yuan.liang.s4@dc.tohoku.ac.jp

Citation:

Yuan, L., Ohtani, E., Ikuta, D., Kamada, S., Tsuchiya, J., Naohisa, H., … Suzuki, A. (2018). Chemical reactions between Fe and H_2O up to megabar pressures and implications for water storage in the Earth's mantle and core. *Geophysical Research Letters*, *45*, 1330–1338. https://doi.org/10.1002/2017GL075720

Received 22 SEP 2017
Accepted 26 JAN 2018
Accepted article online 29 JAN 2018
Published online 8 FEB 2018

Chemical Reactions Between Fe and H_2O up to Megabar Pressures and Implications for Water Storage in the Earth's Mantle and Core

Liang Yuan[1], Eiji Ohtani[1,2], Daijo Ikuta[1], Seiji Kamada[1], Jun Tsuchiya[3], Hirao Naohisa[4], Yasuo Ohishi[4], and Akio Suzuki[1]

[1]Department of Earth and Planetary Material Sciences, Tohoku University, Sendai, Japan, [2]V.S. Sobolev Institute of Geology and Mineralogy, Siberian Branch, Russian Academy of Sciences, Novosibirsk, Russia, [3]Geodynamics Research Center, Ehime University, Matsuyama, Japan, [4]Japan Synchrotron Radiation Research Institute, Sayo, Japan

Abstract We investigated the phase relations of the Fe-H_2O system at high pressures based on in situ X-ray diffraction experiments and first-principles calculations and demonstrate that FeH*x* and FeO are present at pressures less than ~78 GPa. A recently reported pyrite-structured FeO_2 was identified in the Fe-H_2O system at pressures greater than ~78 GPa after laser heating. The phase observed in this study has a unit cell volume 8%–11% larger than that of FeO_2, produced in the Fe-O binary system reported previously, suggesting that hydrogen might be retained in a FeO_2H_x crystal structure. Our observations indicate that H_2O is likely introduced into the deep Earth through reaction between iron and water during the accretion and separation of the metallic core. Additionally, reaction between Fe and H_2O would occur at the core-mantle boundary, given water released from hydrous subducting slabs that intersect with the metallic core. Accumulation of volatile-bearing iron compounds may provide new insights into the enigmatic seismic structures observed at the base of the lower mantle.

1. Introduction

The Earth's core is mainly composed of iron. However, the density of the core, as revealed by seismological observations, is lower than that of pure iron at the corresponding conditions (Birch, 1952). It is therefore invoked that light elements are potentially important ingredients in the core. Among the light elements, hydrogen tends to be excluded as one of the important components in the core due to its high volatility and low solubility in iron at ambient pressure, despite the fact that it is a cosmochemically abundant element. Experiments and thermodynamic calculations suggest that significant amount of hydrogen can be dissolved into iron at high pressures (Antonov et al., 1998; Badding et al., 1991; Fukai, 1984). During accretion and core formation, reaction between iron and water may produce FeH*x*, thus incorporating significant amounts of hydrogen into the core (Badding et al., 1992; Ohtani et al., 2005; Okuchi, 1997). Reaction between iron and water would also be expected at the core-mantle boundary (CMB), as recent studies indicate that hydrous phases may be stable at deepest lower mantle conditions (Ohira et al., 2014; Sano et al., 2008; Suzuki et al., 2000; Walter et al., 2015).

Interest in both the Fe-H and Fe-O binary systems has been enhanced by the recent discoveries of new high-pressure forms of iron hydrides and iron oxides. Experiments and first-principles calculations have suggested that a series of iron hydrides, for example, FeH (dhcp, hcp, and fcc) (Hirao et al., 2004; Isaev et al., 2007; Narygina et al., 2011), FeH_2 (tetragonal), FeH_3 (cubic), and FeH_5 (tetragonal) (Pépin et al., 2014, 2017) could be stabilized at high pressures in the Fe-H system. Iron oxides with complex crystal structures develop in the Fe-O binary system as well under extreme conditions. Beyond the three, well-known, simple iron oxides, that is, $Fe_{1-x}O$ wüstite, Fe_3O_4 magnetite, and Fe_2O_3 hematite, there is a growing number of experimental studies that have identified new high-pressure and high-temperature iron oxides, such as *h*-Fe_3O_4 (Fei et al., 1999), Fe_4O_5 and Fe_5O_6 (Lavina et al., 2011; Lavina & Meng, 2015), and Fe_7O_9 (Sinmyo et al., 2016) that could be stable at conditions relevant to the Earth's interior. The iron peroxide FeO_2, with a pyrite structure (space group $Pa\overline{3}$), was found to be stable at high pressures (Weerasinghe et al., 2015) and was recently synthesized through the reaction between hematite (Fe_2O_3) and oxygen (O_2) (Hu et al., 2016). Further studies suggest that goethite (α-FeOOH) would transform into a pyrite-type phase, a hydrogen-bearing iron peroxide FeO_2Hx (with *x* from 0 to 1), with losing certain amount of hydrogen (Hu et al., 2017;

Table 1
Experimental Conditions and Results of the Reaction Between Fe and H_2O

	Pressure (GPa)			
Run	Before heating	After heating	Temperature (K)	Phases
KA7_001	55	65	2,090 (260)[d]	FeO (B1, B8), $FeHx$ (hcp, dhcp) (Al_2O_3, δ-AlOOH)
MEM_004	70	69	1,694 (100)	FeO (B1, B8), $FeHx$ (hcp, dhcp), H_2O (Al_2O_3, W)
MEM_003	70	69	Quench	FeO (B1, B8), $FeHx$ (hcp, dhcp), H_2O (Al_2O_3, W)
CCTS_002[a]	78	74	1,721 (100)	FeO (B1, B8), $FeHx$ (hcp, dhcp), H_2O (W)
CCTS_005[a]	78	74	Quench	FeO (B1, B8), $FeHx$ (hcp, dhcp), H_2O (W)
TS2_002	82	78	1,700 (100)	FeO (B1, B8), FeO_2Hx, $FeHx$ (hcp, dhcp), H_2O (Al_2O_3, W)
TS3_003	82	78	2,000 (100)	FeO (B1, B8), FeO_2Hx, $FeHx$ (hcp, dhcp), H_2O (Al_2O_3, W)
TS4_004	82	78	Quench	FeO (B1, B8), FeO_2Hx, $FeHx$ (hcp, dhcp), H_2O (Al_2O_3, W)
ccts3_003	90	85	1,790 (100)	FeO (B1, B8), FeO_2Hx, $FeHx$ (dhcp), H_2O (Al_2O_3, W)
ccts3_002	90	85	Quench	FeO (B1, B8), FeO_2Hx, $FeHx$ (dhcp), H_2O (Al_2O_3, W)
ccts2_002	98	115	1,700 (200)	$FeHx$ (hcp), FeO_2Hx (Al_2O_3, W)
ccts2_003	98	115	2,000 (200)	$FeHx$ (hcp), FeO_2Hx (Al_2O_3, W)
ccts2_004	98	115	2,400 (200)	$FeHx$ (hcp), FeO_2Hx (Al_2O_3, W)
ccts2_005	98	115	Quench	$FeHx$ (hcp), FeO_2Hx (Al_2O_3, W)
CCKN_004[b]	105	113	2,000 (160)	FeO_2Hx, $FeHx$ (hcp, dhcp), H_2O, (W, WHx)
CCKN_006[b]	105	113	2,060 (160)	FeO_2Hx, $FeHx$ (hcp, dhcp), H_2O, (W, WHx)
CCKN_005[b]	105	113	Quench	FeO_2Hx, $FeHx$ (hcp, dhcp), H_2O, (W, WHx)
CCT_001[c]	100	97	2,000 (100)[d]	FeO_2Hx, H_2O, (W)

[a] SiO_2 loaded as thermal insulator was not detected during experiments. [b] No thermal insulator was loaded. [c] Starting materials were hematite (Fe_2O_3) and water. [d] Phases in parenthesis indicate materials (SiO_2 or Al2O_3) used as thermal insulator and gasket identified by XRD.

Zhu et al., 2017) or without loss of any hydrogen (Nishi et al., 2017) at pressures $>$70–80 GPa upon laser heating.

The Fe-H_2O system was studied at pressures below 84 GPa and revealed that iron oxide FeO and iron hydride $FeHx$ are the stable run products (Ohtani et al., 2005). Recent studies reported that hydrogen-bearing iron peroxide FeO_2Hx is also stable in the same system at higher pressures (Liu et al., 2017; Mao et al., 2017). The diverse populations of high-pressure iron compounds (iron oxides, iron hydrides, hydrogen-bearing iron peroxides, etc.) make it desirable to constrain the stable-phase assemblages in the Fe-H_2O system in an expanded pressure range. Here by using in situ X-ray diffraction (XRD) observations and first-principles calculations, we have examined the chemical reactions between iron and water in a wide pressure–temperature range to clarify the phase relations in the Fe-H_2O system.

2. Methods

Iron powder and liquid water were compressed to the target pressures using diamond anvil cells and then laser heated to target temperatures. In situ synchrotron powder XRD experiments were performed at BL10XU of Spring-8, Japan (Ohishi et al., 2008). We also conducted first-principles calculations to examine the transition of stable run products from FeO + FeH to FeO_2H + Fe. See supporting information for details of methods.

3. Results and Discussion

The phase relations of the Fe-H_2O system were investigated at pressure-temperature conditions of 65–115 GPa and 1,700–2,400 K. The experimental conditions and results are summarized in Table 1. In addition to the phases formed from starting materials initially loaded into the sample chamber, most XRD patterns contain diffraction lines from thermal insulators (if used), as well as contributions from tungsten gaskets.

At pressures $<$78 GPa, we found that FeO and $FeHx$ were the stable run products of the reaction between iron and water, which is consistent with the results of Ohtani et al. (2005). At pressures between 78 GPa and 85 GPa, we found iron oxide FeO coexisting with the iron peroxide FeO_2Hx (Hu et al., 2016). The iron peroxide FeO_2Hx adopts the crystal structure of pyrite FeS_2 (space group $Pa\bar{3}$) and its unit cell volumes are 8%–11% larger than that of anhydrous FeO_2 synthesized from $Fe_2O_3 + O_2$ (Hu et al., 2016). These features are consistent with hydrogen being dissolved in the crystal structure of FeO_2 and FeO_2Hx. Note that a more recent investigation showed that FeOOH, with a pyrite structure, could be stable in the lower mantle (Nishi et al., 2017). At pressures >85 GPa, FeO_2Hx, and FeHx (hcp or dhcp) were readily indexed as the stable run products. Our observations agree with the results of Mao et al. (2017) and Liu et al. (2017), where FeO_2Hx was synthesized from the reactions between iron/iron oxides (Fe, FeO, Fe_2O_3, etc.) and water (H_2O). However, the FeO_2Hx in our study has larger unit cell volumes compared to that of previous studies (Figure 2a), which might be interpreted as the results of different starting materials and experimental temperature conditions.

The in situ XRD patterns obtained at 113 GPa clearly showed diffraction peaks that can be unambiguously assigned to a simple cubic symmetry with a $Pa\overline{3}$ space group (Figure 1a). All the symmetry-allowed spots for $Pa\overline{3}$-structured FeO_2Hx were present. FeO_2Hx developed sharp diffraction lines within 15 min, and its peaks grew over a 90 min laser heating. The intensities of the diffraction lines from H_2O (ice X), however, did not decline significantly. After temperature quenching, we checked the whole sample chamber by scanning the X-ray beam, and FeO_2Hx was found as the dominant phase. While H_2O (ice X) remained due to the large volume of water, as comparison to the initial iron, loaded into the sample chamber. The experiments were kept at pressure for 2 weeks and a second round of XRD analyses was conducted. Interestingly, we found that the unit cell volume of the tungsten gasket obviously expanded in certain area, which probably was induced by the incorporation of hydrogen. We speculate that free hydrogen was formed during laser heating and it dissolved into the tungsten gasket within this limited time duration; a Raman spectroscopy analysis on this sample could not detect the existence of free hydrogen.

At pressures between 85 GPa and 78 GPa, the FeO_2Hx displayed relatively weak diffraction lines compared to that at 113 GPa although the fitted unit cell volumes matched with that of recent experimental results and theoretical calculations (Hu et al., 2017; Nishi et al., 2017). The diffraction lines developed by FeO_2Hx completely disappeared at pressures 65 GPa, 69 GPa, and 74 GPa.

In one further experiment, we compressed hematite (Fe_2O_3) and water to 97 GPa and laser heated it to ~2,000 K for ~30 min. XRD showed that the pyrite-structured FeO_2Hx formed, indicating the following reaction: $Fe_2O_3 + H_2O \rightarrow FeO_2Hx$.

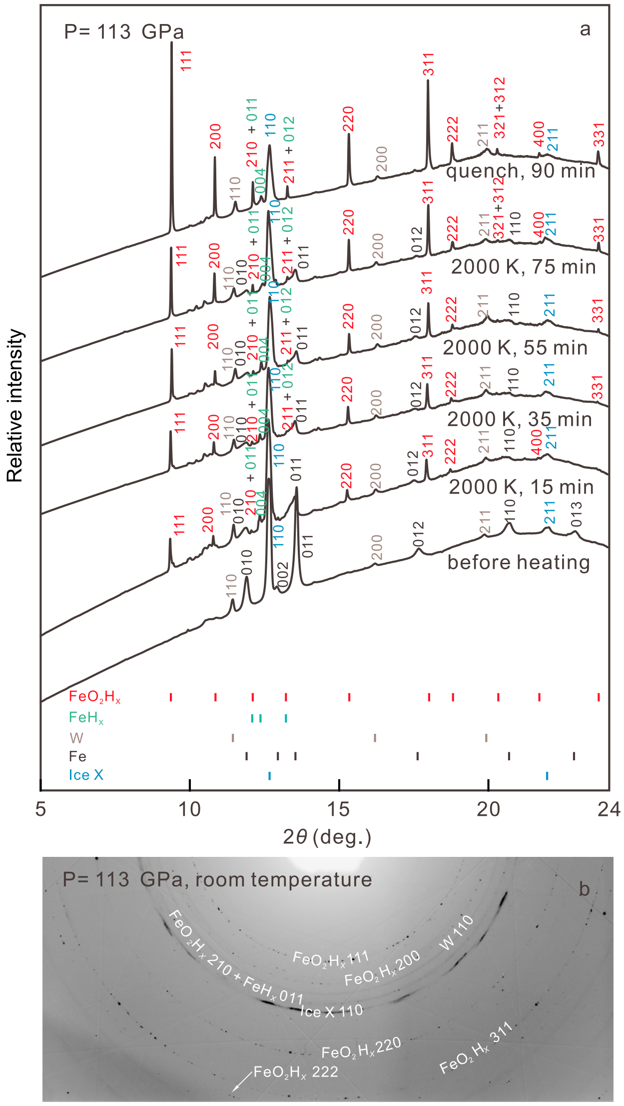

Figure 1. (a) XRD patterns at 113 GPa. (b) A two-dimensional XRD image at 113 GPa after laser-heating.

Hu et al. (2017) found that the volumes of pyrite-structured FeO_2 produced from the dehydration of goethite FeOOH are larger than that of pure FeO_2 synthesized via the reaction between Fe_2O_3 and O_2 in the pressure range of 71–133 GPa. An obvious scattering of the compression data was attributed to the variable nonstoichiometric composition. The volume of FeO_2Hx in this study is also 8%–11% larger than that of pure FeO_2 grown from the $Fe_2O_3 + O_2$ system (Hu et al., 2016) (Figure 2a). Assuming that the volume of FeO_2Hx expands linearly in proportion to the amount of hydrogen dissolved in interstitial sites, the hydrogen concentration in this iron compound can be estimated, based on the following formula (Hu et al., 2017):

$$x = \left[V_{x,\,\mathrm{exp}} - V_{0,\,\mathrm{exp}}\right] / \left[V_{1,\,\mathrm{cal}} - V_{0,\,\mathrm{cal}}\right] \qquad (1)$$

where $V_{x,\ \mathrm{exp}}$ is the observed volume of FeO_2Hx, $V_{0,\ \mathrm{exp}}$ is the volume of pure FeO_2 synthesized in the Fe_2O_3-O_2 system (Hu et al., 2016), and $V_{1,\ \mathrm{cal}}$, and $V_{0,\ \mathrm{cal}}$ denote the volume of FeO_2H and FeO_2 calculated from first-principles methods (Nishi et al., 2017). Our experimentally determined volumes for FeO_2Hx are bracketed by the calculated values given by Nishi et al. (2017) and are comparable to the experimental results from

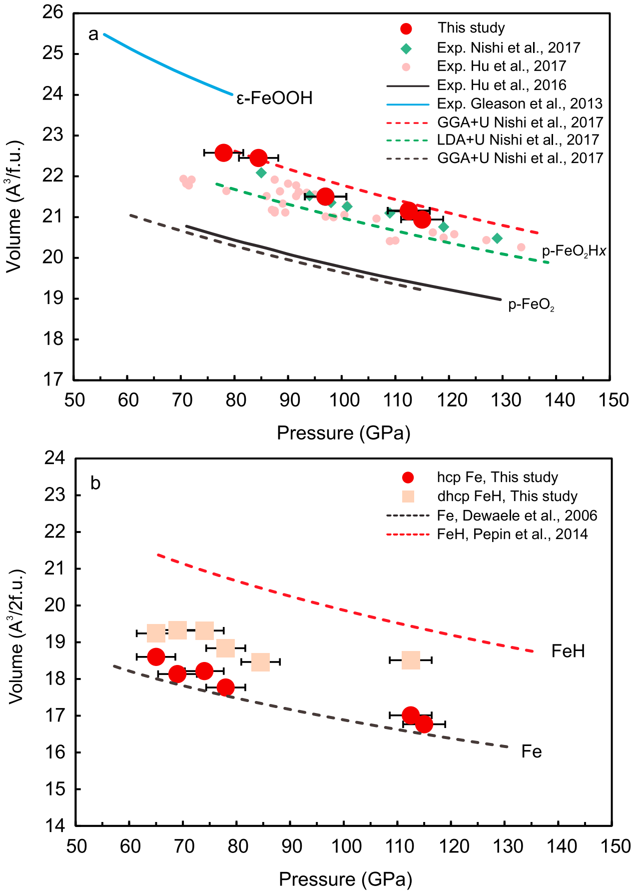

Figure 2. (a) The pressure-volume relations for FeO_2Hx of this study (red circles). Experimental data of pyrite FeO_2Hx are from Hu et al. (2017) (pink circles) and Nishi et al. (2017) (green diamonds), pyrite FeO_2 from Hu et al. (2016) (black solid line), ε-FeOOH from Gleason et al. (2013) (blue solid line). Theoretical data of FeO_2Hx are from Nishi et al. (2017) (red and green dashed lines correspond to generalized gradient approximation (GGA) and local density approximation (LDA) results), FeO_2 from Nishi et al. (2017) (black dashed line). (b) The pressure-volume relations for hcp FeH*x* (circles) and dhcp FeH*x* (squares) of this study. Compressibility curves of pure iron (Dewaele et al., 2006) and FeH (Pépin et al., 2014) were used as baselines to evaluate water contents. All the experimental data are collected at 300 K.

previous studies (Hu et al., 2017; Nishi et al., 2017). Using the two baselines of FeO_2 and FeO_2H (Nishi et al., 2017), the mole fraction of hydrogen for FeO_2Hx in our study is in the range of 0.79–1.00. It was suggested that up to ~50% hydrogen would be released during the phase transition of ε-FeOOH to pyrite-structured FeO_2H (Zhu et al., 2017). The mechanism of dehydrogenation was ascribed to the breakdown of symmetrized hydrogen bonds during the structural transition. Whereas Nishi et al. (2017) suggested that ε-FeOOH directly transforms into pyrite-structured FeO_2H without losing hydrogen, indicating the hydrogen concentration *x* is likely to be unity for FeO_2Hx. Our calculated hydrogen contents in FeO_2Hx are systematically higher than that in Liu et al. (2017), where *x* is in the range of 0.50–0.70. Most experimental data, for example, unit cell volumes and sound velocities, related to FeO_2Hx in previous studies were based on experiments where iron oxides (FeO, Fe_2O_3, etc.) and water (H_2O) were used as starting materials (Hu et al., 2017; Liu et al., 2017; Mao et al., 2017). These systems are more oxidized compared to the Fe-H_2O system explored in this study. We speculate that differences of oxygen fugacity may contribute to the various hydrogen contents in FeO_2Hx among different studies.

Our volume-pressure data of dhcp FeH*x* and hcp FeH*x* are plotted in Figure 2b. A coexistence of hcp FeH*x* and dhcp FeH*x* in the Fe-H system at high pressures was also suggested by Fukai (1992). Water concentrations in iron hydrides have been investigated according to the formula: $x = [V(\mathrm{FeH}x) - V(\mathrm{Fe})]/\Delta V(\mathrm{H})$ (Ohtani et al., 2009; Terasaki et al., 2012). However, uncertainty exists as to the value of ΔV(H) under high pressures. Here we use the volume difference between the Fe and FeH under various pressures for the full range of *x* from 0 to 1. The amount of hydrogen *x* can thus be expressed as follows:

$$x = [V(\mathrm{FeH}, x) - V(\mathrm{Fe}, 0)]/[V(\mathrm{FeH}, 1) - V(\mathrm{Fe}, 0)] \tag{2}$$

where *V*(FeH, *x*), *V*(Fe,0), and *V*(FeH,1) are the observed volume of hcp FeH*x* or dhcp FeH*x*, the volume of pure hcp Fe from Dewaele et al. (2006) and the volume of dhcp FeH from Pépin et al. (2014). The amount of hydrogen dissolved in the hcp FeH*x* and dhcp FeH*x* is in the range of 0.13–0.32 and 0.41–0.90, respectively.

The effect of pressure on the transition of stable products from FeO + FeH → FeO_2H + FeH can be evaluated based on the volume change of the reaction:

$$2\mathrm{FeO} + \mathrm{FeH} \rightarrow \mathrm{FeO_2H} + 2\mathrm{Fe} \tag{3}$$

Our first-principles calculations indicate that the pyrite-structured FeO_2H + 2Fe has lower enthalpies compared to 2FeO + FeH throughout the explored pressure range of 50–150 GPa (Figure S1 in the supporting information). Previous calculations suggest that ε-FeOOH transforms into the pyrite-structured FeO_2H at around 70 GPa (Nishi et al., 2017). Within the stability field of pyrite-structured FeO_2H, instead of FeO + FeH, the pyrite-structured FeO_2H would become one of the stable run products of Fe + H_2O. Whereas the calculated enthalpy of FeOOH +2Fe is lower than that of 2FeO + FeH at pressures less than 78 GPa. This inconsistency is most likely induced by the exchange-correlation functional used in the calculations. The standard generalized gradient approximation or local density approximation often fails to reproduce the stability of iron oxide systems (e.g., Otte et al., 2011). In addition, uncertainty of pressure measurement, stress in the sample chamber, and kinetics of the reaction may also contribute to the inconsistency between experimental and computational results.

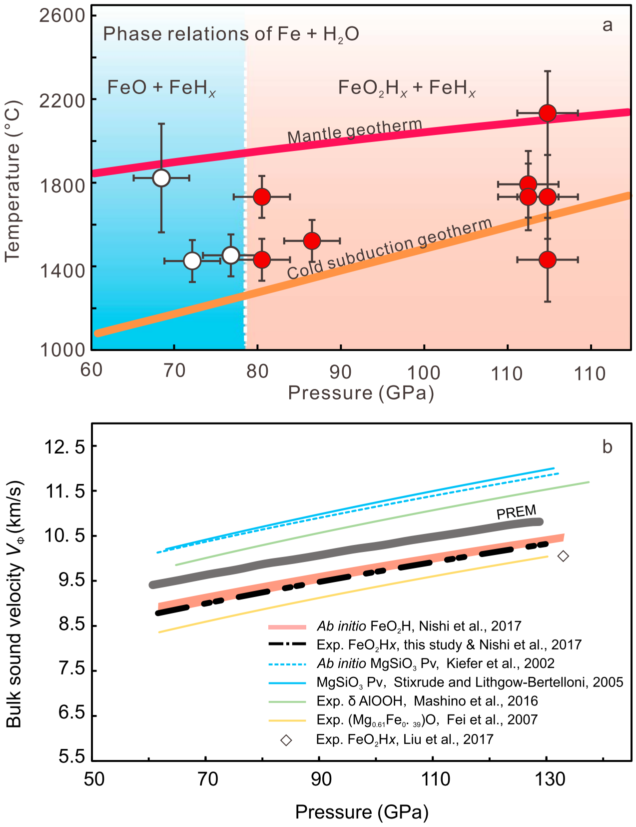

Figure 3. (a) *P-T* phase diagram showing the phases relations of Fe + H_2O. Geotherms for the normal mantle (Brown & Shankland, 1981) and the cold subduction slabs (Kirby et al., 1996) are depicted by thick solid lines. (b) Comparison of bulk sound velocities of FeO_2Hx, $(Mg_{0.61}Fe_{0.39})O$, δ AlOOH, and $MgSiO_3$ bridgmanite. The experimental sound velocity for FeO_2Hx (Liu et al., 2017) is indicated by the diamond symbol. The FeO_2Hx has slower bulk sound velocities compared to the PREM (Dziewonski & Anderson, 1981). Compression data refer to Fei et al. (2007) for $(Mg_{0.61}Fe_{0.39})O$, Mashino et al. (2016) for δ AlOOH, Kiefer et al. (2002) and Stixrude and Lithgow-Bertelloni (2005) for $MgSiO_3$ bridgmanite, and Nishi et al. (2017) and the present study for FeO_2Hx.

At 78 GPa, the molar volume for FeO is 9.04 cm^3/mol (Fischer et al., 2011), FeH is 6.25 cm^3/mol (Pépin et al., 2014), and Fe is 5.28 cm^3/mol (Dewaele et al., 2006). Using the measured volume of 13.60 cm^3/mol for FeO_2H in this work, the reaction has a volume reduction of 0.7%. Pressure lowers the Gibbs free energy of the reaction by $\Delta G = \int \Delta V dP$, thus a transition for the stable run products from $2FeO + FeH \rightarrow FeO_2H + 2Fe$ is likely to occur at high pressures within the stability field of FeO_2H. This volume change, however, tends to become positive as FeO_2H becomes less compressible relative to FeO + FeH at pressures higher than ~100 GPa. The crossover of the volume change, as reproduced by our first-principles calculations (Figure S1), could potentially stabilize FeO + FeH under the deep core conditions.

Phase relations for Fe-H_2O are summarized in the *P-T* phase diagram (Figure 3a). Our experimental results demonstrate that iron and water would react along geotherms of a typical mantle and that for a cold subducting slab (Brown & Shankland, 1981; Kirby et al., 1996). We conclude that FeO + FeH is the stable assemblage $<$78 GPa, whereas FeO_2H + FeH becomes stable $>$78 GPa.

4. Geophysical Implications

Experimental and theoretical studies of FeH*x* suggest that such an iron hydride can satisfy the density and sound velocity of the Earth's core (Hirao et al., 2004; Mao et al., 2004; Sakamaki et al., 2016; Shibazaki et al., 2012; Tagawa et al., 2016). A primary mechanism for including hydrogen into the Earth's core might be through reaction between iron and water during core formation. FeH*x* has a much lower melting temperature than pure iron by several hundreds of degrees (Sakamaki et al., 2009). The dissolution of hydrogen into iron can greatly lower its melting temperature, which might be a prerequisite for efficiently segregating heavy metal from surrounding silicates (Stevenson, 1990). In the shallow mantle, FeO is absorbed into the surrounding silicates, while FeH*x* is considered to be unreactive with surrounding silicates (Ohtani et al., 2005). Due to the strong Fe-H bonding, FeH*x* is unlikely to decompose and can exist in a molten state at increasing temperatures (Badding et al., 1992; Nishi et al., 2017; Okuchi, 1997). Therefore, hydrogen can be stably transported by FeH*x* to great depths in the Earth. With its notably high density (~6.897 g/cm^3 at 113 GPa) in comparison to the density (~5.357 g/cm^3) of surrounding silicates, FeO_2Hx would normally sink into the base of the mantle. However, whether pyrite-structured FeO_2Hx can deliver hydrogen into the deep of the proto-Earth depends on its thermal stability. The present experiment implies a coexistence of FeH*x* and FeO_2Hx at pressure greater than ~80 GPa, which begins to appear in a proto-Earth at a diameter greater than 4,500 km. The unit cell volumes for FeO_2Hx obtained in this study are consistent with that reported by Nishi et al. (2017) and this pyrite phase may be stoichiometric in composition, that is, $x \sim 1$, which indicates very small amount of hydrogen would be released during its transportation to the base of the mantle.

Silicates such as pyroxene, garnet, and Al-bearing bridgmanite at high pressures can incorporate ferric iron (Frost et al., 2004; McCammon, 1997; Rohrbach et al., 2007). Metallic iron could be saturated in the deep mantle because of charge disproportionation where Fe^{2+} (silicates) $\rightarrow$ Fe^{3+} (silicates) + Fe^0 (metal). Experimental evidence is in line with the discovery of metallic iron phases included in natural diamonds presumably originated from the mantle transition zone or uppermost lower mantle (Smith et al., 2016). Note that recently reported aluminous bridgmanite has an unexpected drop of Fe^{3+} content in the midmantle of 1,100 to 1,700 km depths (Shim et al., 2017). The oxidation state change of Fe in bridgmanite will lead to a lower metallic iron content in this region. Metallic iron may play the role of storing large amount of water in the deep mantle as hydrogen was suggested to be favorably partitioned into metallic iron rather than the coexisting silicate mineral (Ohtani et al., 2009). At the top of the lower mantle, dehydration melting would occur when mantle transition zone material is swept down to the lower mantle by mantle convection due to a large contrast of water partitioning between ringwoodite and bridgmanite (Schmandt et al., 2014). Additionally, dense hydrous magnesium phases, for example, superhydrous phase B and phase D, in subducting slabs that are stagnating near 660 km seismic discontinuity might go through hydrous melting (Ghosh & Schmidt, 2014; Ohtani et al., 2003). Dehydration melting of phase δ-H solid solutions would be expected in peridotite system at 60–70 GPa (Walter et al., 2015). The produced hydrous melts would react with the saturated metallic iron producing assemblages of FeH*x* and iron oxides. The aluminous hydrous phase, δ AlOOH, was suggested to be a stable water reservoir in the lower mantle (Sano et al., 2008). At pressures greater than ~78 GPa, δ AlOOH would react with metallic iron to form FeH*x* and FeO_2Hx. However, FeO_2Hx may not exist independently; it is more likely stabilized as a solid solution with δ AlOOH under deep mantle conditions, as revealed by the experiments of Nishi et al. (2017).

The CMB might be a critical location where water can meet with iron and extensive reactions might occur between them (Mao et al., 2017). Postperovskite containing 1–2 wt.% H_2O at *D*″ region was suggested to be stable based on ab initio calculations (Townsend et al., 2015). In the Al-bearing systems, hydrogen favors postperovskite over perovskite with water partition coefficients ranging from 3:1 to 8:1 (Townsend et al., 2016), although the results need to be confirmed experimentally. Hydrous melts or fluids might be generated if hydrous postperovskite is swept by mantle convection through the postperovskite-bridgmanite phase boundary due to potentially high solubility of water in postperovskite and the large contrast in water portioning coefficient between postperovskite and bridgmanite. The hydrous minerals δ AlOOH, phase H $MgSiO_2(OH)_2$, and their solid solutions can be stable up to CMB conditions (Ohira et al., 2014; Sano et al., 2008; Suzuki et al., 2000; Walter et al., 2015). Therefore, water could be transported to the deep lower mantle and core by hydrous phases in cold subducting slabs. However, these hydrous phases are thermally unstable when they are stagnant at the CMB due to the large geothermal gradient on the mantle side of this boundary. The released water (or hydrous melts) can react with the core and likely form the assemblage of FeO_2Hx + FeH*x*. The thermal stability of FeO_2Hx is as yet unknown. FeO_2Hx might be less favored as one of the products of the reaction between δ AlOOH and iron because δ AlOOH has such a wide stability field (Sano et al., 2008) and the dehydration temperatures of δ AlOOH very likely exceed the thermal stability of FeO_2Hx. The δ AlOOH may incorporate significant amounts of Si^{4+} and Mg^{2+} in the lower mantle (Ohira et al., 2014), which may reduce its thermal stability, and therefore, it can dehydrate at much lower temperatures where FeO_2Hx would be stable.

Sound velocity of FeO_2Hx may provide new insights into seismic structure of the ultralow velocity zone. The sound velocities for FeO_2Hx have been measured at 133 GPa, 300 K with *P* waves velocity *V*p = 11.32 km/s and *S* waves velocity *V*s = 4.50 km/s (Liu et al., 2017), which are relatively slower than that in the ambient silicate mantle. In view of the scarcity of experimental elastic data, here we also estimate the bulk sound velocity V_Φ of FeO_2Hx according to the following equation:

$$V_\Phi = (K_S/\rho)^{1/2} \tag{4}$$

where K_S is the adiabatic bulk modulus and ρ is the density. Ks is related to the isothermal bulk modulus, K_T, by $K_S = K_T(1 + \alpha\gamma T) \approx K_T$ at room temperature conditions. K_T and ρ were obtained using the compressibility data of FeO_2Hx from the present study and the data of experiments and first-principles calculations (Nishi et al., 2017). At ~133 GPa, the bulk sound velocity of FeO_2Hx is estimated to be 10.37 km/s, close to 10.06 km/s calculated from the experimental data of Liu et al. (2017). A difference of the bulk sound velocity can be attributed to the different hydrogen contents as incorporation of hydrogen increases V_P whereas decreases V_S of FeO_2Hx (Liu et al., 2017). Oxygen fugacity may control the hydrogen contents in FeO_2Hx, which in turn affect the sound velocities of this phase. The reaction of iron and water explored here might better simulate that occurs at the CMB where metallic iron from the core reacts with fluids released from the slabs at the bottom of the lower mantle. It might become critical to explore the properties of FeO_2Hx under oxidation conditions applicable to the CMB. The bulk sound velocities of FeO_2Hx are slower than that of bridgmanite ($MgSiO_3$) and the preliminary reference Earth model values (Dziewonski & Anderson, 1981) at the base of the lower mantle (Figure 3b). FeO_2Hx thus could be a candidate for the distinct ultralow velocity zone. Furthermore, FeO_2Hx produced at the CMB could be linked to the global scale events, such as the Great Oxidation Event and geodynamic instability of the mantle materials (Mao et al., 2017). Testing these hypotheses must await more studies on its physical and chemical properties, for example, high-temperature sound velocities and thermal stability.

5. Conclusion

We investigated the reaction of H_2O and Fe at deep Earth conditions using in situ X-ray diffraction experiments and first-principles calculations. We found that the stable run products are FeO and FeHx at pressures <78 GPa, and FeO_2Hx and FeHx at pressures >78 GPa. An 8%–11% larger volume than pure FeO_2, indicates that hydrogen is retained in the crystal structure of FeO_2Hx. We suggest that large amount of water might have been introduced into depths during the accretion and separation of the metallic core via iron-water reaction. Reaction between iron and water may also provide new insights into the enigmatic seismic structures at the CMB.

Acknowledgments
We thank T. Sakamaki, F. Maeda, and I. Ohira for their experimental assistance. We thank H. K. Mao for the information on his recent works. Comments from H. K. Mao and an anonymous reviewer have improved this manuscript. This study was supported by the JSPS KAKENHI (grants JP15H05748 to E. O., JP15H05828 to A. S., and JP15H05834 to J. T.). J. T. was also supported in part by MEXT as "Exploratory Challenge on Post-K computer" (Frontiers of Basic Science: Challenging the Limits). E. O. was also partly supported by the Ministry of Education and Science of the Russian Federation (Project 14B25.31.0032). S. K. was partly supported by KAKENHI grants 26247089, 15H05831, and 16K13902. The synchrotron radiation experiments were performed at SPring-8 with the approval of the Japan Synchrotron Radiation Research Institute (Proposals 2016B1494, 2016B1214, 2017A1474, 2017A1251, 2017A1673, 2017B1514, and 2017B169). L. Y. is supported by the International Joint Graduate Program in Earth and Environmental Science (GP-EES), Tohoku University. Experimental data has been shown in Figures 1–3, S1–S3, and Tables 1, S1 and S2.

References

Antonov, V. E., Cornell, K., Fedotov, V. K., Kolesnikov, A. I., Ponyatovsky, E. G., Shiryaev, V. I., & Wipf, H. (1998). Neutron diffraction investigation of the dhcp and hcp iron hydrides and deuterides. *Journal of Alloys and Compounds*, *264*(1-2), 214–222. https://doi.org/10.1016/S0925-8388(97)00298-3

Badding, J., Hemley, R., & Mao, H. (1991). High-pressure chemistry of hydrogen in metals: In situ study of iron hydride. *Science*, *253*(5018), 421–424. https://doi.org/10.1126/science.253.5018.421

Badding, J. V., Mao, H.-K., & Hemley, R. J. (1992). High-pressure crystal structure and equation of state of iron hydride: Implications for the Earth's core. In Y. Syono & M. H. Manghnani (Eds.), *High-pressure research: application to Earth and planetary sciences* (pp. 363–371). Washington, DC: American Geophysical Union.

Birch, F. (1952). Elasticity and constitution of the Earth's interior. *Journal of Geophysical Research*, *57*(2), 227–286. https://doi.org/10.1029/JZ057i002p00227

Brown, J., & Shankland, T. (1981). Thermodynamic parameters in the Earth as determined from seismic profiles. *Geophysical Journal of the Royal Astronomical Society*, *66*(3), 579–596. https://doi.org/10.1111/j.1365-246X.1981.tb04891.x

Dewaele, A., Loubeyre, P., Occelli, F., Mezouar, M., Dorogokupets, P. I., & Torrent, M. (2006). Quasihydrostatic equation of state of iron above 2 Mbar. *Physical Review Letters*, *97*(21), 215504. https://doi.org/10.1103/PhysRevLett.97.215504

Dziewonski, A. M., & Anderson, D. L. (1981). Preliminary reference Earth model. *Physics of the Earth and Planetary Interiors*, *25*(4), 297–356. https://doi.org/10.1016/0031-9201(81)90046-7

Fei, Y., Frost, D. J., Mao, H.-K., Prewitt, C. T., & Haeusermann, D. (1999). In situ structure determination of the high-pressure phase of Fe_3O_4. *American Mineralogist*, *84*(1-2), 203–206. https://doi.org/10.2138/am-1999-1-222

Fei, Y., Zhang, L., Corgne, A., Watson, H., Ricolleau, A., Meng, Y., & Prakapenka, V. (2007). Spin transition and equations of state of (Mg, Fe)O solid solutions. *Geophysical Research Letters*, *34*, L17307. https://doi.org/10.1029/2007GL030712

Fischer, R. A., Campbell, A. J., Shofner, G. A., Lord, O. T., Dera, P., & Prakapenka, V. B. (2011). Equation of state and phase diagram of FeO. *Earth and Planetary Science Letters*, *304*(3-4), 496–502. https://doi.org/10.1016/j.epsl.2011.02.025

Frost, D. J., Liebske, C., Langenhorst, F., & McCammon, C. A. (2004). Experimental evidence for the existence of iron-rich metal in the Earth's lower mantle. *Nature*, *428*(6981), 409–412. https://doi.org/10.1038/nature02413

Fukai, Y. (1984). The iron-water reaction and the evolution of the Earth. *Nature*, *308*(5955), 174–175. https://doi.org/10.1038/308174a0

Fukai, Y. (1992). Some properties of the Fe-H system at high pressures and temperatures, and their implications for the Earth's core. In *High-Pressure Research: Application to Earth and Planetary Sciences* (Vol. 67, pp. 373–385). Washington, DC: TERRAPUB.

Ghosh, S., & Schmidt, M. W. (2014). Melting of phase D in the lower mantle and implications for recycling and storage of H_2O in the deep mantle. *Geochimica et Cosmochimica Acta*, *145*, 72–88. https://doi.org/10.1016/j.gca.2014.06.025

Gleason, A., Quiroga, C., Suzuki, A., Pentcheva, R., & Mao, W. (2013). Symmetrization driven spin transition in ε-FeOOH at high pressure. *Earth and Planetary Science Letters*, *379*, 49–55. https://doi.org/10.1016/j.epsl.2013.08.012

Hirao, N., Kondo, T., Ohtani, E., Takemura, K., & Kikegawa, T. (2004). Compression of iron hydride to 80 GPa and hydrogen in the Earth's inner core. *Geophysical Research Letters*, *31*, L06616. https://doi.org/10.1029/2003GL019380

Hu, Q., Kim, D. Y., Liu, J., Meng, Y., Yang, L., Zhang, D., et al. (2017). Dehydrogenation of goethite in Earth's deep lower mantle. *Proceedings of the National Academy of Sciences of the United States of America*, *114*(7), 1498–1501. https://doi.org/10.1073/pnas.1620644114

Hu, Q., Kim, D. Y., Yang, W., Yang, L., Meng, Y., Zhang, L., & Mao, H.-K. (2016). FeO_2 and FeOOH under deep lower-mantle conditions and Earth's oxygen-hydrogen cycles. *Nature*, *534*(7606), 241–244. https://doi.org/10.1038/nature18018

Isaev, E. I., Skorodumova, N. V., Ahuja, R., Vekilov, Y. K., & Johansson, B. (2007). Dynamical stability of Fe-H in the Earth's mantle and core regions. *Proceedings of the National Academy of Sciences of the United States of America*, *104*(22), 9168–9171. https://doi.org/10.1073/pnas.0609701104

Kiefer, B., Stixrude, L., & Wentzcovitch, R. M. (2002). Elasticity of (Mg,Fe)SiO_3-perovskite at lower mantle conditions. *Geophysical Research Letters*, *29*(11), 1539. https://doi.org/10.1029/2002GL014683

Kirby, S. H., Stein, S., Okal, E. A., & Rubie, D. C. (1996). Metastable mantle phase transformations and deep earthquakes in subducting oceanic lithosphere. *Reviews of Geophysics*, *34*(2), 261–306. https://doi.org/10.1029/96RG01050

Lavina, B., Dera, P., Kim, E., Meng, Y., Downs, R. T., Weck, P. F., et al. (2011). Discovery of the recoverable high-pressure iron oxide Fe_4O_5. *Proceedings of the National Academy of Sciences of the United States of America*, *108*(42), 17,281–17,285. https://doi.org/10.1073/pnas.1107573108

Lavina, B., & Meng, Y. (2015). Unraveling the complexity of iron oxides at high pressure and temperature: Synthesis of Fe_5O_6. *Science Advances*, *1*(5), e1400260. https://doi.org/10.1126/sciadv.1400260

Liu, J., Hu, Q., Kim, D. Y., Wu, Z., Wang, W., Xiao, Y., et al. (2017). Hydrogen-bearing iron peroxide and the origin of ultralow-velocity zones. *Nature*, *551*(7681), 494–497. https://doi.org/10.1038/nature24461

Mao, H. K., Hu, Q., Yang, L., Liu, J., Kim, D. Y., Meng, Y., et al. (2017). When water meets iron at Earth's core-mantle boundary. *National Science Review*, nwx109. https://doi.org/10.1093/nsr/nwx109

Mao, W. L., Sturhahn, W., Heinz, D. L., Mao, H. K., Shu, J., & Hemley, R. J. (2004). Nuclear resonant X-ray scattering of iron hydride at high pressure. *Geophysical Research Letters*, *31*, L15618. https://doi.org/10.1029/2004GL020541

Mashino, I., Murakami, M., & Ohtani, E. (2016). Sound velocities of δ-AlOOH up to core-mantle boundary pressures with implications for the seismic anomalies in the deep mantle. *Journal of Geophysical Research: Solid Earth*, *121*, 595–609. https://doi.org/10.1002/2015JB012477

McCammon, C. (1997). Perovskite as a possible sink for ferric iron in the lower mantle. *Nature*, *387*(6634), 694–696. https://doi.org/10.1038/42685

Narygina, O., Dubrovinsky, L. S., McCammon, C. A., Kurnosov, A., Kantor, I. Y., Prakapenka, V. B., & Dubrovinskaia, N. A. (2011). X-ray diffraction and Mössbauer spectroscopy study of *fcc* iron hydride FeH at high pressures and implications for the composition of the Earth's core. *Earth and Planetary Science Letters*, *307*(3-4), 409–414. https://doi.org/10.1016/j.epsl.2011.05.015

Nishi, M., Kuwayama, Y., Tsuchiya, J., & Tsuchiya, T. (2017). The pyrite-type high-pressure form of FeOOH. *Nature*, *547*(7662), 205–208. https://doi.org/10.1038/nature22823

Ohira, I., Ohtani, E., Sakai, T., Miyahara, M., Hirao, N., Ohishi, Y., & Nishijima, M. (2014). Stability of a hydrous δ-phase, AlOOH–MgSiO$_2$(OH)$_2$, and a mechanism for water transport Into the base of lower mantle. *Earth and Planetary Science Letters*, *401*, 12–17. https://doi.org/10.1016/j.epsl.2014.05.059

Ohishi, Y., Hirao, N., Sata, N., Hirose, K., & Takata, M. (2008). Highly intense monochromatic X-ray diffraction facility for high-pressure research at SPring-8. *High Pressure Research*, *28*(3), 163–173. https://doi.org/10.1080/08957950802208910

Ohtani, E., Hirao, N., Kondo, T., Ito, M., & Kikegawa, T. (2005). Iron-water reaction at high pressure and temperature, and hydrogen transport Into the core. *Physics and Chemistry of Minerals*, *32*(1), 77–82. https://doi.org/10.1007/s00269-004-0443-6

Ohtani, E., Toma, M., Kubo, T., Kondo, T., & Kikegawa, T. (2003). In situ X-ray observation of decomposition of superhydrous phase B at high pressure and temperature. *Geophysical Research Letters*, *30*(2), 1029. https://doi.org/10.1029/2002GL015549

Okuchi, T. (1997). Hydrogen partitioning into molten iron at high pressure: Implications for Earth's core. *Science*, *278*(5344), 1781–1784. https://doi.org/10.1126/science.278.5344.1781

Otte, K., Pentcheva, R., Schmahl, W. W., & Rustad, J. R. (2011). Pressure-induced structural and electronic transitions in FeOOH form first principles. *Physical Review B*, *80*, 205116

Pépin, C., Geneste, G., Dewaele, A., Mezouar, M., & Loubeyre, P. (2017). Synthesis of FeH$_5$: A layered structure with atomic hydrogen slabs. *Science*, *357*(6349), 382–385. https://doi.org/10.1126/science.aan0961

Pépin, C. M., Dewaele, A., Geneste, G., Loubeyre, P., & Mezouar, M. (2014). New iron hydrides under high pressure. *Physical Review Letters*, *113*(26), 265504. https://doi.org/10.1103/PhysRevLett.113.265504

Rohrbach, A., Ballhaus, C., Golla-Schindler, U., Ulmer, P., Kamenetsky, V. S., & Kuzmin, D. V. (2007). Metal saturation in the upper mantle. *Nature*, *449*(7161), 456–458. https://doi.org/10.1038/nature06183

Sakamaki, K., Takahashi, E., Nakajima, Y., Nishihara, Y., Funakoshi, K., Suzuki, T., & Fukai, Y. (2009). Melting phase relation of FeH*x* up to 20 GPa: Implication for the temperature of the Earth's core. *Physics of the Earth and Planetary Interiors*, *174*(1-4), 192–201. https://doi.org/10.1016/j.pepi.2008.05.017

Sakamaki, T., Ohtani, E., Fukui, H., Kamada, S., Takahashi, S., Sakairi, T., et al. (2016). Constraints on Earth's inner core composition inferred from measurements of the sound velocity of hcp-iron in extreme conditions. *Science Advances*, *2*(2), e1500802. https://doi.org/10.1126/sciadv.1500802

Sano, A., Ohtani, E., Kondo, T., Hirao, N., Sakai, T., Sata, N., et al. (2008). Aluminous hydrous mineral δ-AlOOH as a carrier of hydrogen into the core-mantle boundary. *Geophysical Research Letters*, *35*, L03303. https://doi.org/10.1029/2007GL031718

Schmandt, B., Jacobsen, S. D., Becker, T. W., Liu, Z., & Dueker, K. G. (2014). Dehydration melting at the top of the lower mantle. *Science*, *344*(6189), 1265–1268. https://doi.org/10.1126/science.1253358

Shibazaki, Y., Ohtani, E., Fukui, H., Sakai, T., Kamada, S., Ishikawa, D., et al. (2012). Sound velocity measurements in dhcp-FeH up to 70 GPa with inelastic X-ray scattering: Implications for the composition of the Earth's core. *Earth and Planetary Science Letters*, *313*, 79–85.

Shibazaki, Y., Ohtani, E., Terasaki, H., Suzuki, A., & Funakoshi, K.-i. (2009). Hydrogen partitioning between iron and ringwoodite: Implications for water transport into the Martian core. *Earth and Planetary Science Letters*, *287*(3–4), 463–470. https://doi.org/10.1016/j.epsl.2009.08.034

Shim, S.-H., Grocholski, B., Ye, Y., Alp, E. E., Xu, S., Morgan, D., et al. (2017). Stability of ferrous-iron-rich bridgmanite under reducing midmantle conditions. *Proceedings of the National Academy of Sciences of the United States of America*, *114*(25), 6468–6473. https://doi.org/10.1073/pnas.1614036114

Sinmyo, R., Bykova, E., Ovsyannikov, S. V., McCammon, C., Kupenko, I., Ismailova, L., & Dubrovinsky, L. (2016). Discovery of Fe$_7$O$_9$: A new iron oxide with a complex monoclinic structure. *Scientific Reports*, *6*(1), 32852. https://doi.org/10.1038/srep32852

Smith, E. M., Shirey, S. B., Nestola, F., Bullock, E. S., Wang, J., Richardson, S. H., & Wang, W. (2016). Large gem diamonds from metallic liquid in Earth's deep mantle. *Science*, *354*(6318), 1403–1405. https://doi.org/10.1126/science.aal1303

Stevenson, D. J. (1990). Fluid dynamics of core formation. In H. E. Newsom & J. E. Jones (Eds.), *Origin of the Earth* (pp. 231–250). New York: Oxford University Press.

Stixrude, L., & Lithgow-Bertelloni, C. (2005). Thermodynamics of mantle minerals—I. Physical properties. *Geophysical Journal International*, *162*(2), 610–632. https://doi.org/10.1111/j.1365-246X.2005.02642.x

Suzuki, A., Ohtani, E., & Kamada, T. (2000). A new hydrous phase δ-AlOOH synthesized at 21 GPa and 1000 C. *Physics and Chemistry of Minerals*, *27*(10), 689–693. https://doi.org/10.1007/s002690000120

Tagawa, S., Ohta, K., Hirose, K., Kato, C., & Ohishi, Y. (2016). Compression of Fe–Si–H alloys to core pressures. *Geophysical Research Letters*, *43*, 3686–3692. https://doi.org/10.1002/2016GL068848

Terasaki, H., Ohtani, E., Sakai, T., Kamada, S., Asanuma, H., Shibazaki, Y., et al. (2012). Stability of Fe–Ni hydride after the reaction between Fe–Ni alloy and hydrous phase (δ-AlOOH) up to 1.2 Mbar: Possibility of H contribution to the core density deficit. *Physics of the Earth and Planetary Interiors*, *194*, 18–24.

Townsend, J. P., Tsuchiya, J., Bina, C. R., & Jacobsen, S. D. (2015). First-principles investigation of hydrous post-perovskite. *Physics of the Earth and Planetary Interiors*, *244*, 42–48. https://doi.org/10.1016/j.pepi.2015.03.010

Townsend, J. P., Tsuchiya, J., Bina, C. R., & Jacobsen, S. D. (2016). Water partitioning between bridgmanite and postperovskite in the lowermost mantle. *Earth and Planetary Science Letters*, *454*, 20–27. https://doi.org/10.1016/j.epsl.2016.08.009

Walter, M., Thomson, A., Wang, W., Lord, O., Ross, J., McMahon, S., et al. (2015). The stability of hydrous silicates in Earth's lower mantle: Experimental constraints from the systems $MgO–SiO_2–H_2O$ and $MgO–Al_2O_3–SiO_2–H_2O$. *Chemical Geology*, *418*, 16–29. https://doi.org/10.1016/j.chemgeo.2015.05.001

Weerasinghe, G. L., Pickard, C. J., & Needs, R. (2015). Computational searches for iron oxides at high pressures. *Journal of Physics Condensed Matter*, *27*(45), 455501. https://doi.org/10.1088/0953-8984/27/45/455501

Zhu, S. C., Hu, Q., Mao, W. L., Mao, H. K., & Sheng, H. (2017). Hydrogen-bond symmetrization breakdown and dehydrogenation mechanism of FeO_2H at high pressure. *Journal of the American Chemical Society*, *139*(35), 12,129–12,132. https://doi.org/10.1021/jacs.7b06528